Effect of Premixed Fuel Preparation for Partially Premixed Combustion with a Low Octane Gasoline on a Light-Duty Multi-Cylinder Compression Ignition Engine

Adam B. Dempsey*, Scott Curran, & Robert Wagner
Oak Ridge National Laboratory
Fuels, Engines, and Emissions Research Center
National Transportation Research Center
2360 Cherahala Blvd.
Knoxville, TN 37932

William Cannella
Chevron Energy Technology Company
6001 Bollinger Canyon Road
San Ramon, CA 94583

*Corresponding Author
Email: dempsab@gmail.com

Abstract

Gasoline compression ignition concepts with the majority of the fuel being introduced early in the cycle are known as partially premixed combustion (PPC). Previous research on single- and multi-cylinder engines has shown that PPC has the potential for high thermal efficiency with low NOx and soot emissions. A variety of fuel injection strategies has been proposed in the literature. These injection strategies aim to create a partially stratified charge to simultaneously reduce NOx and soot emissions while maintaining some level of control over the combustion process through the fuel delivery system. The impact of the direct injection strategy to create a premixed charge of fuel and air has not previously been explored, and its impact on engine efficiency and emissions is not well understood. This paper explores the effect of sweeping the direct injected pilot timing from -91° to -324° ATDC, which is just after the exhaust valve closes for the engine used in this study. During the sweep, the pilot injection consistently contained 65% of the total fuel (based on command duration ratio), and the main injection timing was adjusted slightly to maintain combustion phasing near top dead center. A modern four cylinder, 1.9 L diesel engine with a variable geometry turbocharger, high pressure common rail injection system, wide included angle injectors, and variable swirl actuation was used in this study. The pistons were modified to an open bowl configuration suitable for highly premixed combustion modes. The stock diesel injection system was unmodified, and the gasoline fuel was doped with a lubricity additive to protect the high pressure fuel pump and the injectors. The study was conducted at a fixed speed/load condition of 2000 rpm and 4.0 bar brake mean effective pressure (BMEP). The pilot injection timing sweep was conducted at different intake manifold pressures, swirl levels, and fuel injection

pressures. The gasoline used in this study has relatively high fuel reactivity with a research octane number of 68. The results of this experimental campaign indicate that the highest brake thermal efficiency and lowest emissions are achieved simultaneously with the earliest pilot injection timings (i.e., during the intake stroke).

Introduction

In an effort to reduce NOx and soot emissions in-cylinder from compression ignition engines, while improving thermal efficiency to meet challenging fuel economy regulations, many new compression ignition combustion strategies have been proposed. These combustion strategies are known as low temperature combustion (LTC) and produce simultaneous reductions in NOx and soot emissions. Simply speaking, the goal of the LTC process is to achieve sufficient premixing between the fuel and air to avoid soot formation and to maintain low combustion temperatures to avoid NOx formation, which is achieved through premixing and dilution.

One of the first and most straightforward methods of achieving LTC is homogeneous charge compression ignition (HCCI) combustion. HCCI combustion has been researched for many years and was initially studied in four-stroke engines by Najt and Foster [1]. The HCCI process essentially involves a completely premixed fuel/air charge that is inducted into the cylinder at equivalence ratios that are typically lean ($\sim \Phi < 0.5$). Once within the cylinder, the mixture is compressed until autoignition occurs.

HCCI combustion has been shown to have superior characteristics in terms of thermal efficiency, which result from lower heat transfer losses and shorter combustion durations compared to diesel combustion. In addition, the dilute, low temperature combustion process yields near zero NOx and soot emissions. However, HCCI operation has demonstrated challenges with its operable load range, combustion controllability, high pressure rise rates (i.e., engine noise), and combustion efficiency, stemming from incomplete combustion with high unburned hydrocarbon (UHC) and carbon monoxide (CO) emissions.

Partially premixed combustion (PPC) is a concept that aims to address the aforementioned challenges associated with fully premixed compression ignition combustion. PPC is a hybrid between HCCI and conventional diesel combustion (CDC). To avoid high NOx and soot formation rates, the fuel must have sufficient time to mix with the air before ignition takes place to ensure locally dilute (i.e., lean) combustion. In the case of PPC, the fuel is injected early during the compression stroke to promote fuel/air mixing before ignition and to avoid high NOx and

soot formation rates, while still maintaining some coupling between the start of fuel injection and the start of combustion.

Gasoline-type fuels are excellent candidates for PPC operation because of their high resistance to autoignition (high octane number) and their high volatility, which allows for early direct injections or port injections without severe wall wetting. Using gasoline in compression ignition engines for low NOx and soot emissions has been investigated by a number of researchers over the last decade, from which several operating strategies have emerged.

Researchers at Lund University have developed a gasoline compression ignition (GCI) operating strategy using gasoline-type fuels with a variety of octane numbers on a heavy-duty engine [2], [3]. Their operational strategy uses a single or double injection, with the main injection event relatively close to top dead center. For low- to mid-engine loads, the main injection event is separated from the start of combustion by 5 to 10 crank angle degrees, which results from the low reactivity of the gasoline fuels. This results in low soot emissions. However, to yield ultralow NOx emission levels (less than 0.3 g/kW-hr), exhaust gas recirculation (EGR) rates of ~50% and a global equivalence ratio of ~0.6 were still required in those studies. It is challenging for state-of-the-art air-handling systems to provide globally lean equivalence ratios and high EGR rates (e.g., 40% and greater) [4], [5]. This type of gasoline compression ignition strategy has been investigated by Ciatti et al. on a light-duty multi-cylinder engine over the entire operating range [6].

Other researchers have been investigating gasoline PPC strategies that are significantly more fuel premixed [7], [8], [9], [10]. With these types of strategies the majority of the total fuel is premixed, either through port fuel injection, fumigation, or very early direct injections. The remainder of the fuel is direct injected during the latter half of the compression stroke. This injection strategy creates a slight amount of equivalence ratio stratification and relatively low peak equivalence ratios. This tends to lessen the EGR requirement to achieve low NOx emissions, while soot is inherently low because of the premixed nature. The disadvantage of these “majority-premixed” PPC concepts is the ability to achieve high loads because of high pressure rise rates and combustion phasing controllability because of the low levels of fuel stratification [11].

The current study investigates gasoline PPC operation using a double direct injection strategy on a multi-cylinder, light-duty diesel engine using a piston designed for highly premixed combustion concepts. There is no fumigation or port fuel injection. The focus is on characterizing the effect of varying the pilot (i.e., first) injection

timing to understand the impact on thermal efficiency and emissions. The pilot injection timing was varied from -91° to 324° ATDC, which is just after the exhaust valve closes for the engine used in this study. During the pilot timing sweep, the fraction of the total fuel in the pilot injection was kept constant at 65%, which is based on command duration ratios, and the main injection was varied slightly to maintain the combustion phasing near top dead center. The pilot injection timing sweep was conducted at different intake manifold pressures, swirl levels, and fuel injection pressures. The investigation focused on a 2000 RPM, 4.0 bar BMEP operating point, which is approximately 20% of peak load for the base engine, and comparisons are made to a Euro IV calibration at the same operating condition.

Experimental Engine & Laboratory Setup

The engine used for this study was a modified 2007 GM direct injection 1.9 L diesel engine. The base engine geometric specifications are shown in Table 1. The original equipment manufacturer (OEM) pistons were replaced with pistons that are more suited for highly premixed combustion concepts. The modified piston bowl geometry was designed for dual-fuel operation (i.e., reactivity controlled compression ignition) using detailed computational fluid dynamics (CFD) modeling [12]. The modified piston features a wide/shallow bowl geometry, which creates a more quiescent combustion chamber and reduces the piston crown surface area compared to the OEM re-entrant bowl geometry. Thus, it is expected that this piston bowl shape would be optimal for majority premixed single-fuel gasoline PPC as well. Using single-cylinder engine experiments, the modified piston bowl geometry yielded an increase in the combustion efficiency and indicated efficiency for dual-fuel operation compared to the OEM piston at a matched compression ratio using a variety of fuels [13].

Table 1: Geometric specifications of a model year 2007 GM 1.9 L compression ignition engine.

Number of cylinders	4
Bore [mm]	82.0
Stroke [mm]	90.4
Connecting rod length [mm]	145.4
Modified compression ratio [-]	15.1
Total displacement [L]	1.9
Intake valve open (IVO)* [°ATDC]	344°
Intake valve close (IVC)* [°ATDC]	-132°
Exhaust valve open (EVO)* [°ATDC]	116°
Exhaust valve close (EVC)* [°ATDC]	-340°

*Valve timings taken at 0.1 mm valve lift.

In this work, the modified piston uses a reduced compression ratio of 15.1 compared to the stock 17.1 to allow for higher load operation during premixed combustion. A schematic drawing and photograph of the stock OEM piston and the modified piston bowl geometries are shown in Figure 1.

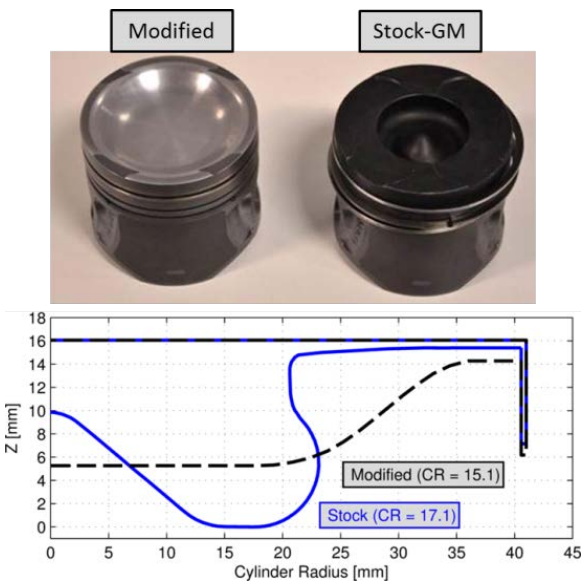

Figure 1: Stock GM 1.9 L piston compared to the modified piston.

The common rail direct injection (DI) system and variable geometry turbocharger (VGT) were left in production form. An aftermarket charge air cooler (CAC) was installed. Figure 2 shows the overall engine and fuel system layout, and Table 2 shows the injector specifications for the common rail DI injectors. The Bosch CRI2.2 injector is a production, high pressure, solenoid-driven, common rail fuel injector that was mounted vertically and in the center of each cylinder. A seven-hole, mini-sac injector tip was used, which has an included angle of 148° (16° down-angle from the fire deck, i.e., the bottom surface of the cylinder head).

The engine is equipped with four variable swirl actuators (VSA): one for each cylinder. The swirl ratio is controlled by throttling one of the intake ports for each cylinder while the other port is completely unthrottled. When the throttled port is fully open, the swirl ratio is at its minimum of ~2.0. By fully closing the throttle, the swirl ratio can be increased to ~5.0.

The stock engine control unit was replaced with a full-pass control system from National Instruments - Powertrain Controls Group (formerly Drivven, Inc.), which allowed simultaneous control of each DI injector, allowing for cylinder-to-cylinder balancing as well as all other relevant engine parameters, such as rail pressure, VGT position, and VSA position.

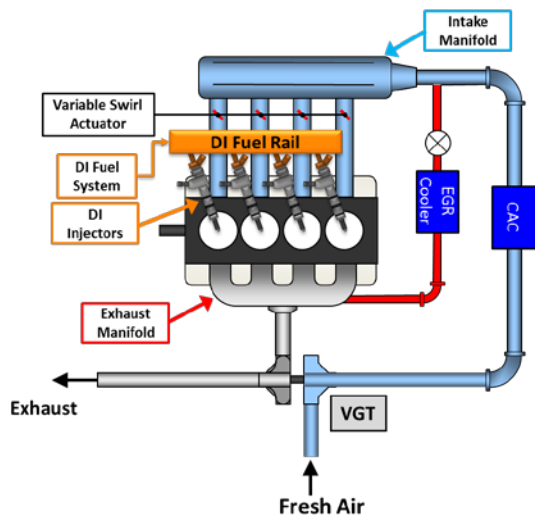

Figure 2: Multi-cylinder GM 1.9 L engine schematic. The DI injectors are shown on an angle for illustrative purposes but are mounted vertically in the cylinder head.

Table 2: Common rail direct injector specifications.

Model	Bosch CRI2.2
Number of holes [-]	7
Hole size [mm]	0.14
Included spray angle [deg.]	148°

The DI fuel system was left in the stock form except that the polymer injector return lines were replaced with stainless steel leading to the stock damper. Since the DI fuel system was not designed for high volatility fuels, extra care was taken to prevent fuel vapor from forming in the system or potential cavitation before the fuel meter or high pressure pump. A Max Machinery 710 Fuel Measurement system was used to supply fuel to the Bosch CP1 high pressure fuel pump at ~4.15 bar. The Max Machinery 710 fuel system consists of a fuel conditioning and measurement package. The fuel conditioner contains a vapor eliminator along with regulators, internal heat

exchangers, level controller, and lift pump. Heat exchangers were added to the supply and return lines, which were cooled using an external chiller set to 15°C. A copper coil was wrapped around the high pressure fuel rail, which was supplied 15°C coolant from the chiller. A schematic of the fuel system is shown in Figure 3.

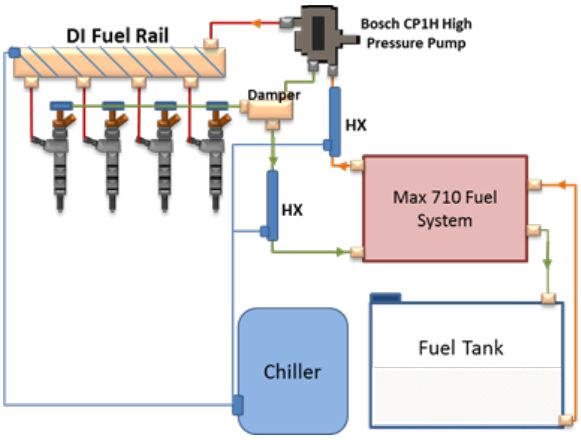

Figure 3: Fuel system configuration for measurement and conditioning for high pressure direct injection of gasoline.

The Max Machinery 710 fuel system has a positive displacement volumetric flow measurement system, which was used to record the instantaneous fuel flow to the engine. The intake fresh air flow rate was measured using a laminar flow element. Conditioned air was supplied to the engine at a constant temperature of 25°C and a relative humidity of 60%.

High-speed in-cylinder pressure data were acquired using Kistler model 6058A pressure transducers installed in the glow plug ports of all four cylinders. Individual Kistler type 5010 dual-mode amplifiers were used to process the pressure signals and the built-in combustion package from National Instruments/Drivven was used to process the data. Combustion metrics were monitored and recorded using the Drivven combustion analysis toolkit (DCAT). Cylinder pressure was pegged to the intake manifold pressure near the end of the intake stroke and sampled at a resolution of 0.2 crank angle degrees. High-speed data (i.e., in-cylinder pressure) was recorded for 300 consecutive engine cycles. The low-speed data (air flow, fuel flow, boundary conditions, and emissions) were recorded for 180 seconds at ~2 Hz.

In a multi-cylinder engine there are variations in conditions from cylinder to cylinder, such as wall temperature, EGR level, trapped residuals, total fuel delivered, etc. Kinetically controlled combustion strategies like PPC are especially sensitive to changes in these types of parameters. This can lead to significant cylinder to cylinder imbalances in the combustion phasing (CA50), indicated mean effective pressure (IMEP), peak pressure rise rate (PPRR), and emissions. To adjust for these variations and maintain a nearly constant combustion phasing and load

from each cylinder, the total fueling and start of injection commands (SOIc) were varied independently for each cylinder. The DI injection durations needed to be varied by a maximum of 6% from cylinder to cylinder. The SOIcs needed to be varied by a maximum of 2 crank angle degrees. Throughout this study the maximum variability in cylinder-to-cylinder IMEP and CA50 was 7% and 1.5 crank angle degrees, respectively.

Three different indicated cycles will be presented. The gross cycle is comprised of the compression and expansion strokes only (-180° to 180° ATDC, where 0° ATDC represents top dead center of the compression stroke). The net cycle is made up of the entire four-stroke cycle (-360° to 360° ATDC). Lastly, the pumping cycle consists of the exhaust and intake strokes (180° to -180° ATDC), which is the difference between the net and gross cycles.

Exhaust emissions were measured using standard gaseous emissions analyzers. A heated flame ionization detector was used to measure total unburned hydrocarbons (UHC). The UHC emissions are reported on a C1-basis. A heated chemiluminescence analyzer was used to measure total NOx emissions (NO + NO2). Both CO and CO2 were measured using non-dispersive infrared (NDIR) instruments. Intake and exhaust O2 were measured using a paramagnetic detector (PMD). The exhaust sample stream was conveyed from heated filters to the instruments through heated lines maintained at 190°C. An AVL 415S smoke meter was used to measure the filter smoke number (FSN), which is an indicator of black carbon containing soot in the exhaust. For all the operating conditions studied here, the FSN was consistently 0.00 and thus will not be reported further.

The emissions analyzers, fuel flowmeter, and air flowmeter were used to calculate three independent air/fuel ratios, as outlined in reference [14]. The aim is for these air/fuel ratios to be in agreement, which ensures data quality and provides a check of the accuracy of the individual measurement devices. In this work, the three air/fuel ratios agreed to within 4% for all the data points recorded.

The fuel used in this study was a nonconventional gasoline with relatively high fuel reactivity (i.e., lower octane number than market gasoline). The volatility characteristics are similar to those of a conventional gasoline. In this study, the fuel was additized with a lubricity additive to protect the high pressure fuel pump and the injectors. The fuel properties are shown in Table 3.

Low octane gasolines, like the fuel used in this study, have been investigated with advanced combustion concepts such as HCCI and GCI [3], [15]. Low octane gasoline fuels for compression ignition engines are attractive for a variety of reasons. From a fuel production standpoint, some lower octane streams are present in refineries, but are usually upgraded to produce higher octane market gasolines. The use of lower octane gasolines could require

less refinery octane upgrading and thus in theory could be a bit less expensive to manufacture and produce less CO2 emissions during production [16]. From an engine combustion standpoint, the lower octane gasoline fuels have been shown to cover a wider operating range for GCI operation while yielding lower combustion noise than conventional, higher octane gasolines [17]. Finally, for more premixed strategies, the ignition delay of low octane gasolines has been shown to be sensitive to the mixture equivalence ratio, thus allowing fuel stratification to be a potential method to control the timing and rate of heat release [15].

Table 3: Low octane gasoline fuel properties.

Density [g/cc]	0.7147
Lower heating value [MJ/kg]	44.38
Molar H/C ratio	2.143
Research octane number (RON)	68
Motored octane number (MON)	66

Experimental Operating Conditions

The current study characterizes gasoline “majority-premixed” PPC using a modern multi-cylinder light-duty compression ignition engine. The focus was to understand the impact of the pilot direct injection timing, which aims to premix the majority of the fuel. The pilot start of injection command (PSOIc) was varied from 91° to 324° ATDC, which is just after the exhaust valve closes for the engine used in this study. The remainder of the fuel was delivered in a later main injection (i.e., double injection strategy). The engine operating conditions for this study are shown in Table 4.

Table 4: Engine operating conditions for pilot injection timing study. Settings shown in bold and italics are referred to as the base settings.

Engine speed [rpm]	2000
Engine load (BMEP) [bar]	4.0 ± 0.05
Intake manifold pressure [bar]	1.05, ***1.15***, 1.25
Intake manifold temperature [°C]	32°
External EGR [%]	0%
Swirl ratio [-]	2.0, ***2.5***, 3.0
Pilot injection timing (PSOIc) [°ATDC]	-324° to -90°
Total fuel in pilot injection* [%]	65%
Main injection timing (SOIc) [°ATDC]	-40° to -30°
Common rail injection pressure [bar]	400, ***550***, 700

*Based on command duration ratios.

Throughout the study the engine speed was held at 2000 rpm, and the engine load was maintained at 4.0 ± 0.05 bar BMEP. The pilot injection timing sweep was conducted at various intake manifold pressures, swirl ratios, and injection pressures, as shown in Table 4. The base settings for these parameters are shown in bold and italics. When a given engine parameter was being swept, the other parameters were kept at their base setting. The engine was consistently operated with 0% EGR, and the intake manifold was maintained at 32°C. The engine coolant and oil temperatures were maintained at 89°C.

The percentage of the total fuel that was delivered in the pilot injection was kept constant at 65%, which is based on injector command durations. However, injector testing has shown that the injector used in this study has a nonlinear response in fuel flow as a function of command duration, up to a command duration of ~0.6 ms [14]. The command durations used in this study were between 0.3 and 0.8 ms. The actual pilot fuel percentage is believed to be higher, and injector flow bench testing suggests that it is ~85% for the operating conditions studied here [14].

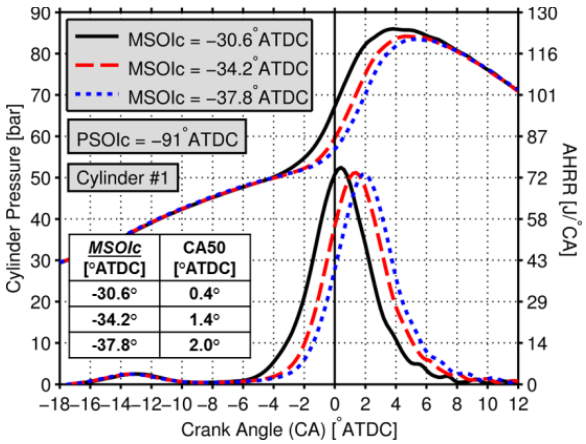

Figure 4: Response of combustion phasing (CA50) to changes in the main injection timing for a pilot injection timing of -91° ATDC. Base settings: Swirl ratio of 2.5, intake pressure of 1.15 bar, and injection pressure of 550 bar.

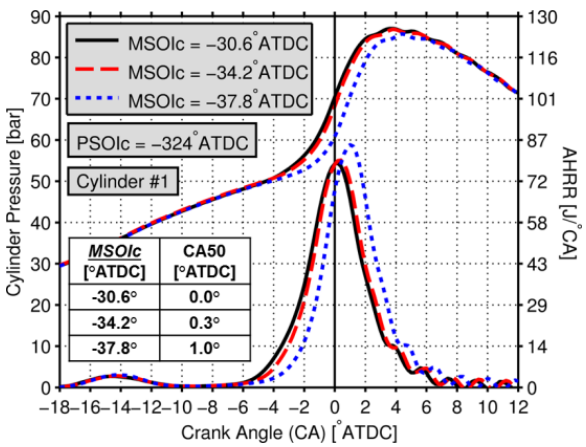

Figure 5: Response of combustion phasing (CA50) to changes in the main injection timing for a pilot injection timing of -324° ATDC. Base settings: swirl ratio of 2.5, intake pressure of 1.15 bar, and injection pressure of 550 bar.

The main start of injection command (MSOIc) was varied between -40° and -30° ATDC to maintain combustion phasing (CA50) near top dead center (-1° to 1° ATDC). As the pilot injection was advanced, the combustion tended to advance as well. To compensate, the main injection timing was advanced. Figure 4 and Figure 5 illustrate the effect of the main injection timing on the combustion phasing (CA50) for the most retarded and most advanced pilot timings, respectively. As shown in the figures, by advancing the main injection, the combustion phasing tends to retard and thus can be used to compensate for the advancement in combustion phasing as the pilot injection is advanced. Throughout this study, as the pilot injection was advanced from -91° to -324° ATDC, the main injection was advanced as well from approximately -30° to -40° ATDC.

Table 5 shows the effect of varying the main injection timing on the NOx, HC, and CO emissions for the two extremes of the pilot injection timing spectrum. As the main injection is advanced, the NOx emissions are reduced significantly (~70% reduction). This is because of the longer mixing period between the end of injection and start of combustion, which will result in lower peak equivalences during the combustion event, and thus lower peak temperatures and lower NOx formation rates. On the contrary, the HC and CO emissions are relatively unaffected by the main injection timing. These results will be important when deciphering the impact of the pilot injection timing considering that the main injection is varied simultaneously.

Table 5: Response of NOx, HC, and CO emissions to changes in the main injection timing for a pilot injection timing of -91° and -324° ATDC. Base settings: swirl ratio of 2.5, intake pressure of 1.15 bar, and injection pressure of 550 bar.

	MSOIc [°ATDC]		
PSOIc = -91° ATDC	**-30.6°**	**-34.2°**	**-37.8°**
BSNOx [g/kW-hr]	0.59	0.27	0.19
BSHC [g/kW-hr]	17.3	18.4	18.9
BSCO [g/kW-hr]	20.6	22.5	22.0
PSOIc = -324° ATDC			
BSNOx [g/kW-hr]	0.69	0.38	0.17
BSHC [g/kW-hr]	11.9	12.7	12.9
BSCO [g/kW-hr]	22.6	23.1	24.4

Figure 6 shows the pilot injection timings considered in this work along with the intake valve lift, exhaust valve lift, cylinder pressure from the baseline condition, and the range of main start of injection commands that were used in this study. As shown in the figure, two of the pilot timings take place after the intake valve has shut on the compression stroke, and four of the timings are during the intake stroke.

The common rail direct injector features a wide included angle (i.e., umbrella angle), which will target the cylinder liner for direct injections earlier than -30° ATDC. Figure 6 shows the spray axis for one of the injector holes and the piston location for the pilot injection timings used in this study. As shown in the figure, by using the wide included angle injector, there will be very little interaction between the fuel injection events (both pilot and main) and the piston bowl.

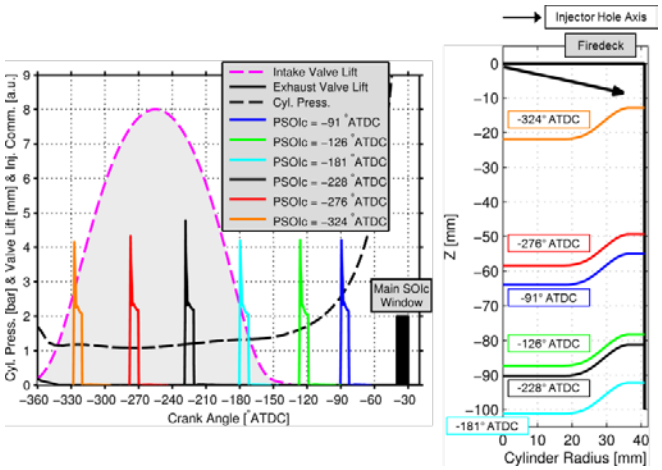

Figure 6: (Left) Illustration of the relationship between pilot start of injection timings and the intake valve lift. (Right) Injector hole spray axis and piston locations for the pilot injection timings.

Pilot Timing Sweep at Various Swirl Ratios

Using the base settings for all other engine operating parameters, the pilot injection timing sweep was conducted at three different in-cylinder swirl ratios: 2.0, 2.5, and 3.0. Figure 7 shows the main start of injection timings and resultant combustion phasings for cylinder #1 during the pilot injection timing sweep. To maintain combustion phasing near top dead center, the main injection was advanced slightly as the pilot injection was advanced, for the two latest pilot injection timings. The other four pilot injection timings used the same main injection timing of approximately -37° ATDC. These results suggest that there is something fundamentally different about the later injection timings (i.e., after IVC). The trend shown here for the main start of injection timing was consistent throughout the study and thus for the sake of brevity is not shown in each section.

Figure 8 shows the cylinder pressure and apparent heat release rate (AHRR) results from cylinder #1 during the pilot injection sweep at the base settings. The injection schedule (pilot and main injection timings) has little impact on the combustion event. However, as will be shown in the subsequent sections, the injection schedule has a large impact on the emissions.

Figure 9 shows the brake-specific carbon monoxide (BSCO) and hydrocarbon (BSHC) emissions as a function of the pilot injection timing for the three different swirl ratios investigated. There is not a strong correlation between the CO emissions and the pilot injection timing. The highest swirl ratio of 3.0 yields the lowest CO emissions. This could be because of improved late-cycle mixing (i.e., post combustion), but could be the result of global equivalence ratio differences. To achieve the higher swirl ratio, the engine was throttled slightly, which

reduces the air flow and increases the global equivalence ratio for a given fuel flow. For lean, fully premixed combustion, it has been shown that the CO emissions decrease with increasing global equivalence ratio [18]. The nominal global equivalence ratios for the swirl ratios of 2.0 and 3.0 are 0.33 and 0.35, respectively.

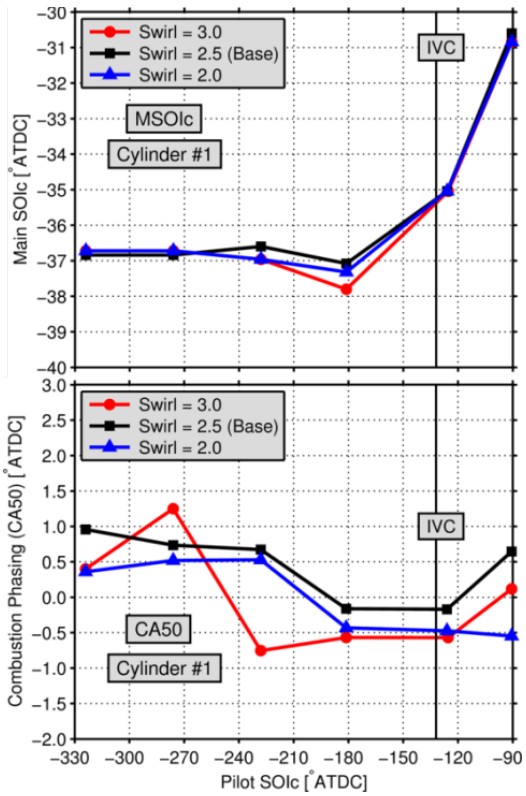

Figure 7: (Top) Main injection timing and (bottom) combustion phasing (CA50) for cylinder #1 as a function of the pilot injection timing for three different swirl ratios. Base settings: intake pressure of 1.15 bar and injection pressure of 550 bar.

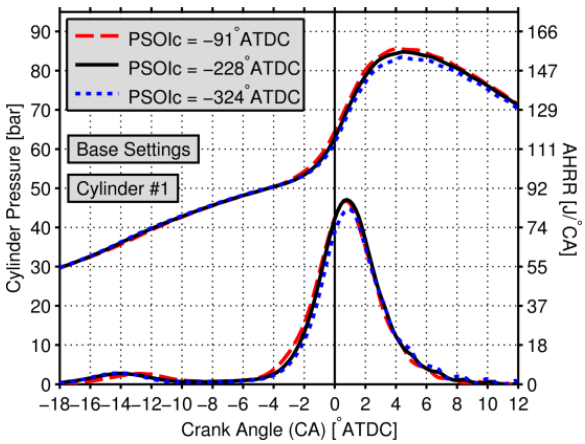

Figure 8: Cylinder pressure and AHRR results from cylinder #1 during the pilot injection timing sweep at the baseline settings. Base settings: swirl ratio of 2.5, intake pressure of 1.15 bar, and injection pressure of 550 bar.

In contrast, the hydrocarbon emissions are strongly correlated with the pilot injection timing. As shown in Figure 9, as the pilot injection is advanced past intake valve close (IVC) and into the intake stroke, the HC emissions are reduced by ~30%. This manifests in nearly a 2.5% absolute improvement in the combustion efficiency over the pilot timing sweep, which can be seen in Figure 10. The swirl ratio has little impact on the HC emissions. In addition, it was shown in Table 5 that the main injection timing variation that is associated with the pilot timing sweep is not responsible for this reduction in the HC emissions. Thus, the HC reduction is because of the advancement of the pilot injection timing.

The significant reduction in the HC emissions as the pilot injection is advanced is thought to be because of the high in-cylinder turbulence levels and thus mixing rates that are generated by the intake process. Research has shown that the in-cylinder mean velocities and turbulence levels are highest during the intake process of an internal combustion engine and quickly decrease after the intake valve shuts [19]. The latest pilot injection timings (-126° and -91° ATDC) occur after the intake valve has closed, when the chamber is expected to be relatively quiescent and mixing rates are low. As depicted in Figure 6, these fuel injection events are going to target the cylinder liner and most likely lead to fuel impingement on the liner, resulting in high HC emissions. On the contrary, the pilot injection timings that occur while the intake valve is open likely experience faster breakup, vaporization, and mixing with the incoming air. Even though these timings target the cylinder liner, they might not impinge on the liner and thus lead to more complete combustion.

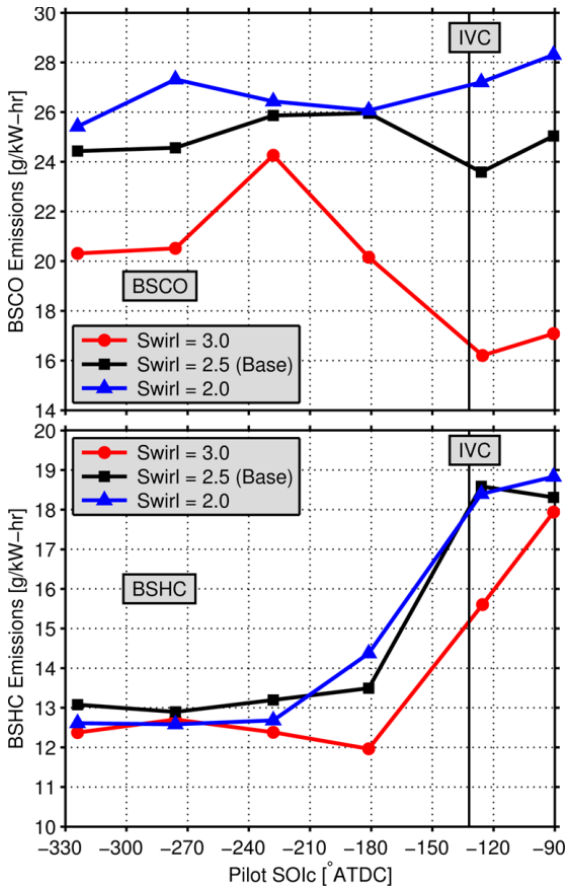

Figure 9: (Top) Brake-specific CO emissions and (bottom) brake-specific HC emissions as a function of the pilot injection timing for three different swirl ratios. Base settings: intake pressure of 1.15 bar and injection pressure of 550 bar.

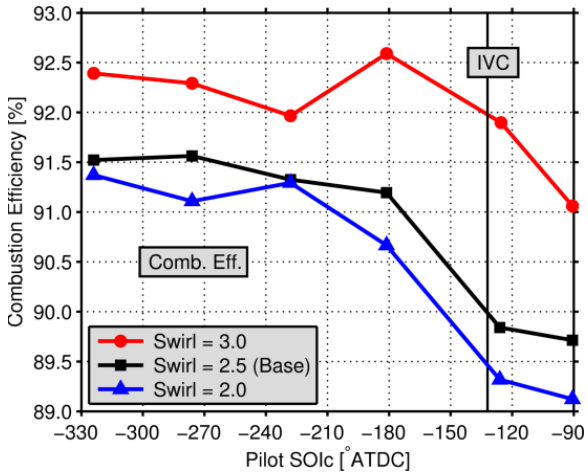

Figure 10: Combustion efficiency as a function of the pilot injection timing for three different swirl ratios. Base settings: intake pressure of 1.15 bar and injection pressure of 550 bar.

Figure 11 shows the brake-specific NOx emissions (BSNOx) as a function of the pilot injection timing for the three swirl ratios investigated in this study. As the pilot injection timing is advanced, the NOx emissions are

reduced significantly, down to ~0.2 g/kW-hr. As discussed previously, the main injection timing was advanced along with the pilot injection to maintain combustion phasing near top dead center. As shown in Table 5, the advancement of the main injection timing is responsible for a major portion of the NOx reduction observed here. However, the potential of the earliest pilot timings to reduce liner impingement could play a role in reducing the NOx emissions as well. Evidence to support this is shown in the injection pressure sweep section.

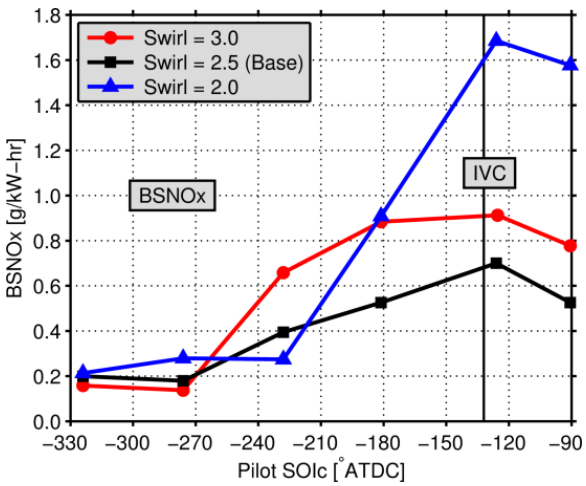

Figure 11: Brake-specific NOx emissions as a function of the pilot injection timing for three different swirl ratios. Base settings: intake pressure of 1.15 bar and injection pressure of 550 bar.

Lastly, Figure 12 shows the variation in brake thermal efficiency (BTE) over the pilot injection sweep for the three different swirl ratios. Despite the higher combustion efficiency for the higher swirl ratio of 3.0, the lower swirl ratio of 2.0 yields the highest BTE. This is because the swirl ratio of 2.0 allows the engine to operate completely unthrottled, which results in globally leaner operation (increased ratio of specific heats) and reduced pumping losses. Additionally, lower swirl ratio has been shown to reduce heat transfer losses and thus increase the thermodynamic efficiency of the engine for premixed LTC [20].

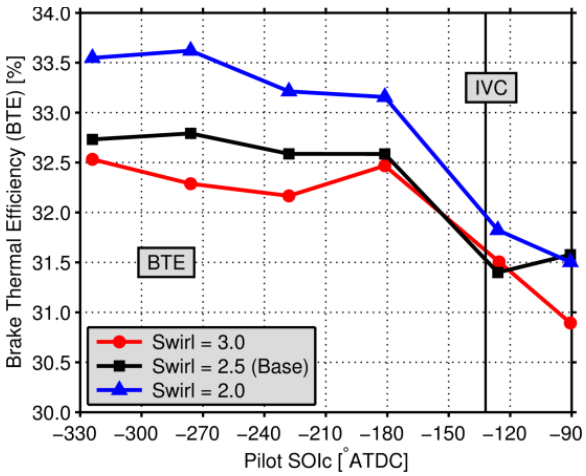

Figure 12: Brake thermal efficiency as a function of the pilot injection timing for three different swirl ratios. Base settings: intake pressure of 1.15 bar and injection pressure of 550 bar.

Pilot Timing Sweep at Various Injection Pressures

Figure 13 shows the BSCO and BSHC emissions as a function of the pilot injection timing for the three different injection pressures investigated. As shown in the figure, there is not a strong correlation between the CO emissions and the pilot injection timing or the injection pressure. However, there is again a ~30% reduction in HC emissions for the early pilot injection timings that occur during the intake process. This result is independent of the injection pressure as well. Figure 14 shows the corresponding increase in the combustion efficiency over the pilot injection sweep. There is a 2.0 to 2.5% absolute improvement in the combustion efficiency for the early pilot injection timings, independent of the injection pressure.

The pilot injection timing of -180° ATDC with an injection pressure of 700 bar produced an average peak pressure rise rate that was too high to allow data to be recorded for any significant period of time (~15 bar/°CA). Thus, this datum is shown as a blank discontinuity on the figures in this section.

Figure 15 shows the NOx emissions over the pilot injection timing sweep for the various injection pressures. As the pilot injection is advanced, the NOx emissions are reduced considerably. Recall, as shown in Table 5, this is partly because of the advancement of the main injection timing as the pilot injection is advanced. However, using 400 bar injection pressure, the three earliest pilot injection timings used the same main injection timing of -36.6° ATDC and had the same CA50 of ~0.5° ATDC. For these cases, the NOx emissions progressively decreased as the pilot injection was advanced, demonstrating some contribution from the pilot injection to the reduction in

NOx emissions. The low injection pressure (400 bar) yields approximately double the NOx emissions compared with the higher injection pressures of 550 and 700 bar. This is because of the longer injection durations and lower mixing rates that will be produced with the lower injection pressure. This will lead to higher peak equivalence ratios at the start of combustion, higher peak temperatures, and thus higher NOx emissions.

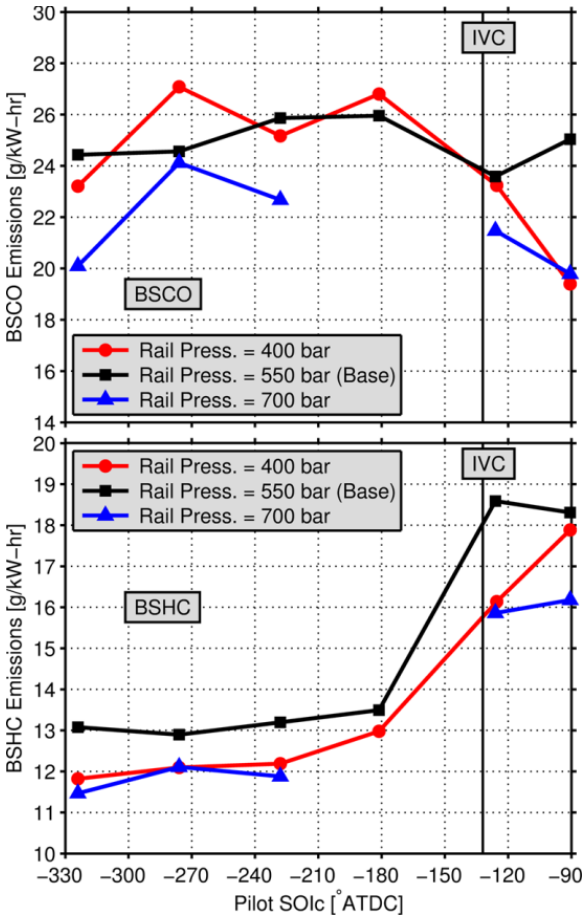

Figure 13: (Top) Brake-specific CO emissions and (bottom) brake-specific HC emissions as a function of the pilot injection timing for three different injection pressures. Base settings: intake pressure of 1.15 bar and swirl ratio of 2.5.

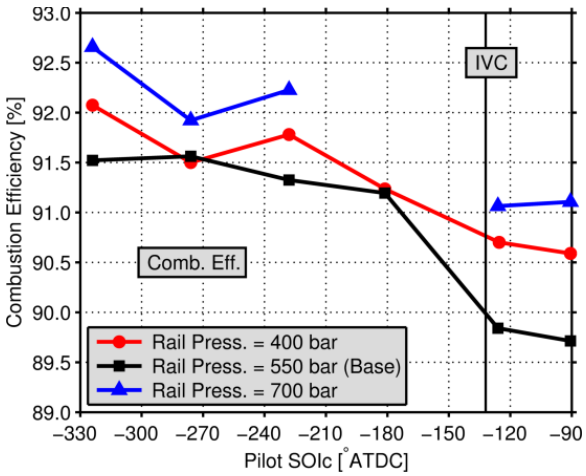

Figure 14: Combustion efficiency as a function of the pilot injection timing for three different injection pressures. Base settings: intake pressure of 1.15 bar and swirl ratio of 2.5.

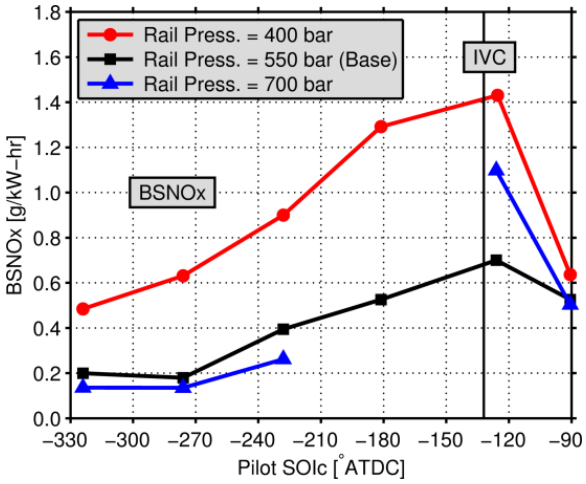

Figure 15: Brake-specific NOx emissions as a function of the pilot injection timing for three different injection pressures. Base settings: intake pressure of 1.15 bar and swirl ratio of 2.5.

Figure 16 shows the brake thermal efficiency as a function of the pilot injection timing for the three different injection pressures. Again, because of the increased combustion efficiency, the earliest pilot injection timings yield the highest brake thermal efficiency. The brake thermal efficiency has a slight dependence on the injection pressure, with the lowest injection pressure yielding slightly higher efficiency. This is thought to be because the high pressure fuel pump is driven by the engine and is a parasitic loss. However, the parasitic losses from the high pressure fuel pump are difficult to quantify with the data collected in this work. The highest injection pressure of 700 bar does not fall in line with the trend of parasitic losses because of its higher combustion efficiency.

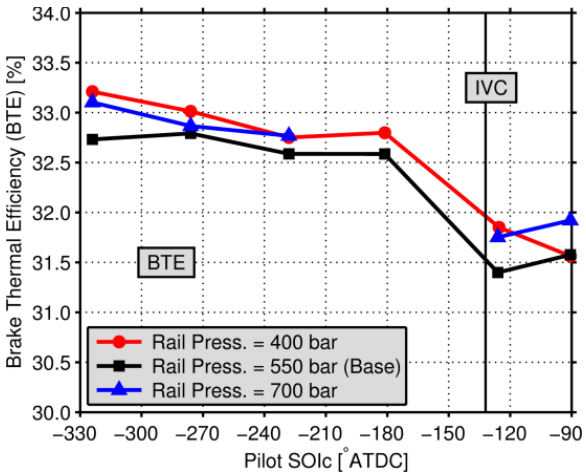

Figure 16: Brake thermal efficiency as a function of the pilot injection timing for three different injection pressures. Base settings: intake pressure of 1.15 bar and swirl ratio of 2.5.

Pilot Timing Sweep at Various Intake Pressures

Finally, the pilot injection timing sweep was conducted at various intake pressures: 1.05, 1.15, and 1.25 bar. Varying the intake pressure on a multi-cylinder engine with a VGT indirectly varies a wide range of parameters that impact the combustion process and the engine efficiency. To achieve the various intake pressures, the exhaust turbine changes its geometry (i.e., aspect ratio). To achieve a higher intake pressure, the turbine vanes progressively close which increases the velocity of the gases flowing over the turbine and in turn produces more turbo-shaft work to drive the compressor wheel. However, this increases the exhaust manifold pressure upstream of the turbine housing (i.e., backpressure). Table 6 shows the variation of exhaust pressure, ratio of intake-to-exhaust pressure, pumping mean effective pressure (PMEP), air/fuel ratio, global equivalence ratio (Φ), and gross indicated mean effective pressure (IMEP) for the three intake pressures investigated in this study. As the intake pressure increases, the exhaust backpressure increases at a nonlinear rate. This results in a progressively lower ratio of intake-to-exhaust pressure and higher PMEP. Therefore to maintain the BMEP at 4.0 bar over the sweep, the fueling rate and IMEP were increased as the intake pressure increased.

Table 6: Engine operating conditions as a result of conducting intake pressure sweep. Indicated cycle work calculated from the average of all four cylinders.

	P_{int} = 1.05 [bar]	**P_{int} = 1.15 [bar]**	**P_{int} = 1.25 [bar]**
$P_{exhaust}$ [bar]	1.16	1.36	1.65
$P_{intake}/P_{exhaust}$ [-]	0.91	0.85	0.76
PMEP [bar]	0.24	0.36	0.56
Air/Fuel Ratio [-]	42.9	44.7	47.3
Global Φ [-]	0.349	0.335	0.316
IMEP [bar]	5.2	5.4	5.6

The final anomaly with the intake pressure sweep is the impact the progressive decrease in the ratio of intake-to-exhaust pressure has on trapped residuals and the combustion process. The lower the intake-to-exhaust pressure ratio is, the higher the amount of trapped exhaust residuals, which will in turn increase the trapped mass temperature at the start of compression. Figure 17 shows the response of combustion phasing (CA50) to changes in the intake pressure, and thus trapped residuals, for a pilot injection timing of 324° ATDC. The main injection timings for the intake pressures of 1.05, 1.15, and 1.25 bar were -32.6°, -36.8°, and 43.2° ATDC, respectively. As shown in the figure, the combustion phasing advances when the intake pressure is increased, despite advancing the main injection timing, which was shown previously to retard the combustion phasing.

This advancement of the combustion phasing is thought to be from the increase in hot trapped residuals as the intake pressure increases and not to the pressure sensitivity of the low octane gasoline's autoignition chemistry. Dec et al. showed that a similar low octane gasoline exhibits very little pressure sensitivity for fully premixed and partially stratified combustion [15]. Nevertheless, even though the combustion phasing was unable to be held constant during the intake pressure sweep, the findings are still useful to understand the impact on multi-cylinder engine performance for gasoline PPC operation.

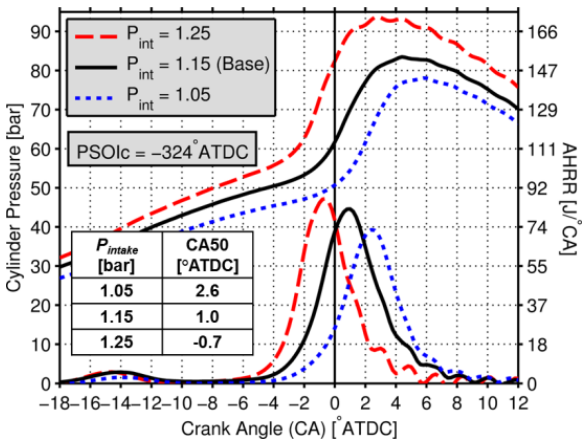

Figure 17: Response of combustion phasing (CA50) to changes in the intake pressure for a pilot injection timing of -324° ATDC. Base settings: swirl ratio of 2.5 and injection pressure of 550 bar.

Figure 18 shows the CO and HC emissions during the pilot injection timing sweep for the various intake pressures. As discussed previously in the section on varying swirl ratio, the CO emissions for premixed combustion tend to decrease with increasing global equivalence ratio [18]. Table 6 shows that as the intake pressure increases, the global equivalence ratio decreases. Thus, it is expected that the lowest intake pressure would yield lower CO emissions, as shown in Figure 18, which is in spite of its retarded combustion phasing, which is shown Figure 17. As shown previously, the hydrocarbon emissions are reduced by ~30% for the advanced pilot injection timings and are not a strong function of the secondary swept parameter, in this case the intake pressure. Figure 19 shows the corresponding increase in the combustion efficiency as the pilot injection is advanced.

Figure 20 shows the NOx emissions during the pilot injection timing sweep for the various intake pressures investigated. The NOx emissions are reduced for the advanced pilot injection timings, but, as discussed earlier, this is partly because of the simultaneous advancement of the main injection timing. Because of the low air/fuel ratio (i.e., high equivalence ratio) for the low intake pressure, the NOx emissions are higher across the entire range of pilot timings. This is attributed to the fact that the combustion is less dilute, which leads to higher combustion temperatures and thus lower CO emissions but higher NOx emissions.

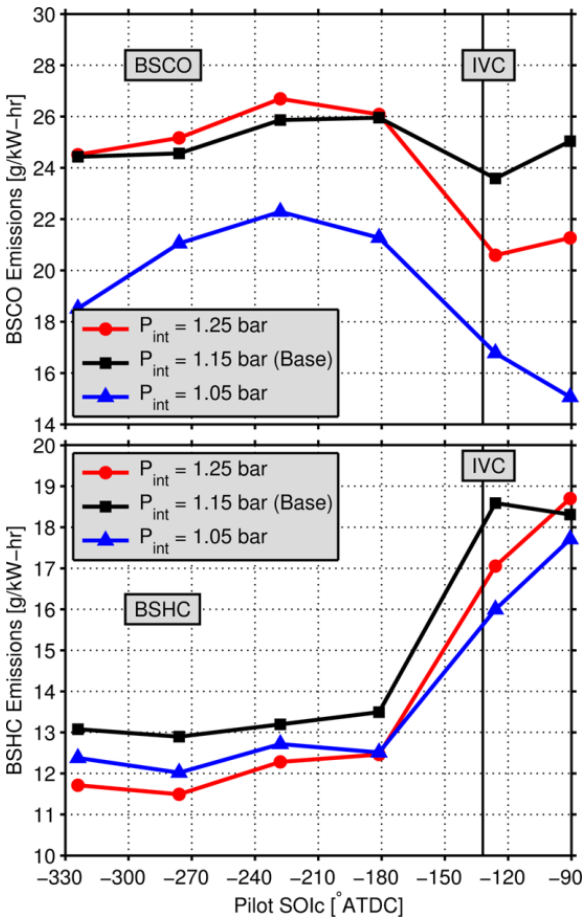

Figure 18: (Top) Brake-specific CO emissions and (bottom) brake-specific HC emissions as a function of the pilot injection timing for three different intake pressures. Base settings: swirl ratio of 2.5 and injection pressure of 550 bar.

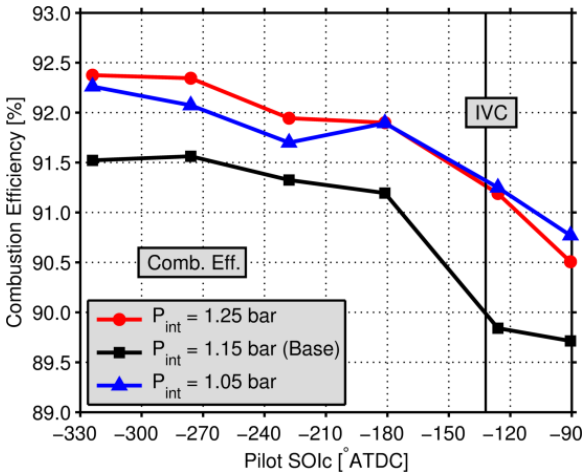

Figure 19: Combustion efficiency as a function of the pilot injection timing for three different intake pressures. Base settings: swirl ratio of 2.5 and injection pressure of 550 bar.

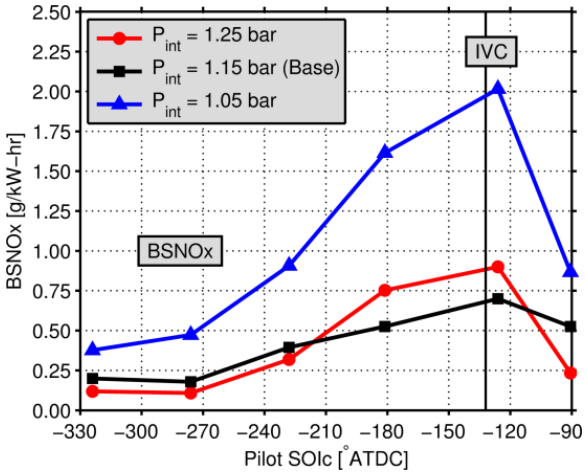

Figure 20: Brake-specific NOx emissions as a function of the pilot injection timing for three different intake pressures. Base settings: swirl ratio of 2.5 and injection pressure of 550 bar.

Figure 21 shows the brake thermal efficiency over the pilot injection timing sweep for the various intake pressures. As the pilot injection is advanced, the brake thermal efficiency increases by 1.0 to 1.5% absolute. This is because of the increase in combustion efficiency, which is shown in Figure 19. However, the intake pressure impacts the BTE to an even greater extent.

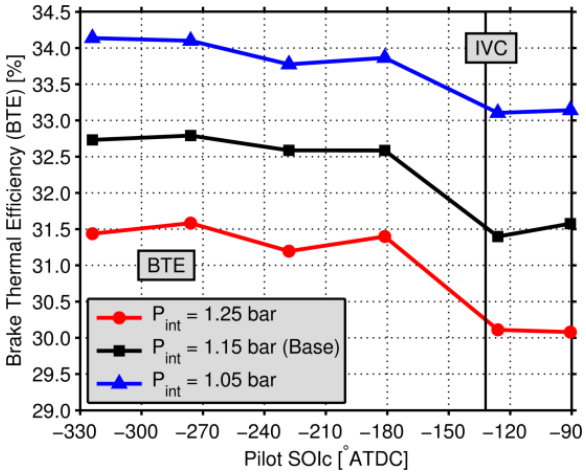

Figure 21: Brake thermal efficiency as a function of the pilot injection timing for three different intake pressures. Base settings: swirl ratio of 2.5 and injection pressure of 550 bar.

Table 7 shows a breakdown of the various engine efficiency metrics. The section on experimental setup outlines the definitions of these different engine cycles. Also note that the indicated efficiencies (i.e., based on cylinder pressure and volume) that are shown in the table include all four cylinders. The cycle work was calculated

for each cylinder individually and then summed to get the total indicated cycle work for the engine. This was divided by the total fuel energy delivered to the engine to determine the cycle efficiency.

As shown in Table 7, the gross indicated efficiency remains relatively constant at ~44% during the intake pressure sweep, despite the many differences between the three operating conditions, such as combustion phasing (Figure 17), air/fuel ratio (Table 6), and combustion efficiency (Figure 19).

However, as shown in Table 6, the pumping requirements for increasing the intake pressure are significant, and thus the net indicated efficiency is reduced from 42.1 to 39.9%, as the intake pressure is increased from 1.05 to 1.25 bar. This additional pumping work is the primary reason why the brake efficiency is highest for the lowest intake pressure. Finally, there is a small frictional benefit (i.e., mechanical efficiency) for the lower intake pressure because the peak cylinder pressures are lower, which directly reduces the engine's frictional losses [21].

Table 7: Summary of overall engine efficiencies over the intake pressure sweep for a pilot injection timing of -324° ATDC. Note that the indicated efficiencies include all four cylinders.

Engine Efficiencies ***[% of fuel energy]***	**P_{int} = 1.05 [bar]**	**P_{int} = 1.15 [bar]**	**P_{int} = 1.25 [bar]**
Gross efficiency [%]	44.1%	44.0%	44.3%
Net efficiency [%]	42.1%	41.0%	39.9%
Pumping efficiency [%] (Net – Gross)	-2.0%	-3.0%	-4.4%
Brake efficiency [%]	34.1%	32.7%	31.4%
Mechanical efficiency [%] (Brake – Net)	-8.0%	-8.3%	-8.5%

Discussion of Results & Convergence on PPC Operating Strategy

In this work it was consistently observed that advancing the pilot injection past bottom dead center and into the intake stroke yielded a ~30% reduction in HC emissions and, in turn, a 2.0 to 2.5% absolute improvement in the combustion efficiency. The CO emissions were relatively unaffected by the pilot injection timing. The NOx emissions consistently decreased with advanced pilot injection timings, but it was concluded that this was at least partly because of a simultaneous advancement of the main injection.

It was found that a low swirl ratio of 2.0 yielded relatively high brake thermal efficiency because the engine is completely unthrottled at this swirl level and most likely reduced heat transfer losses from a more quiescent combustion chamber. Using higher injection pressures (700 bar) resulted in improved combustion efficiency and ultra-low NOx emissions compared with lower injection pressures (400 bar).

The caveats of varying the intake pressure on a multi-cylinder engine with a variable geometry turbocharger were discussed. It was found that low intake pressure (1.05 bar) yields the highest brake thermal efficiency because of reduced pumping work. However, the NOx emissions were relatively high because of the lower dilution level (i.e., lower air/fuel ratio). Low intake pressure could potentially be combined with high injection pressures to maximize efficiency and yield low NOx emissions (less than 0.2 g/kW-hr).

Figure 22 shows the cylinder pressure and AHRR results for all four cylinders using a swirl ratio of 2.0, injection pressure of 700 bar, intake pressure of 1.05 bar, and a pilot and a main injection timing of -324° and -37.8° ATDC, respectively.

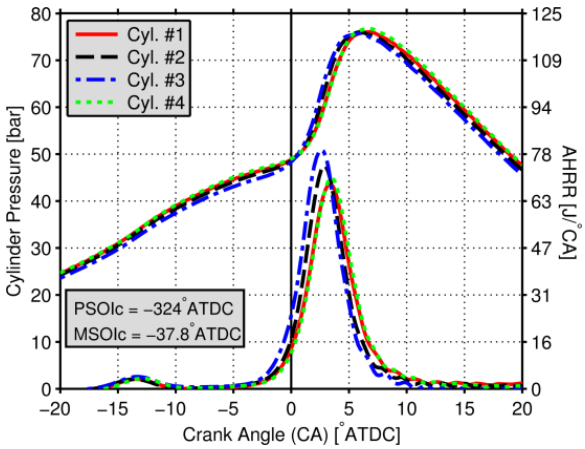

Figure 22: Cylinder pressure and AHRR results for all four cylinders at the final operating condition. Settings: swirl ratio of 2.0, intake pressure of 1.05 bar, and injection pressure of 700 bar.

Table 8: Results from final PPC operating condition at 2000 rpm and 4.0 bar BMEP. Settings: Swirl ratio of 2.0, intake pressure of 1.05 bar, injection pressure of 700 bar, and 0% EGR.

	PPC
CA50 [°ATDC] (min to max)*	2.5° to 3.8°
Gross IMEP [bar] (min to max)*	5.18 to 5.35
COV of IMEP [%] (min to max)*	1.6% to 2.4%
PPRR [bar/°CA] (min to max)*	9.6 to 11.4
Gross efficiency [%]	44.5%
Net efficiency [%]	42.7%
Brake efficiency [%]	34.4%
BSHC [g/kW-hr]	13.1
BSCO [g/kW-hr]	20.6
Combustion efficiency [%]	91.6%
BSNOx [g/kW-hr]	0.18
FSN [-]	0.00

*Min to max are cylinder-to-cylinder for the average cycle.

Table 8 shows the engine performance and emissions results for this final PPC operating condition. The cylinders were well balanced in terms of combustion phasing (CA50) and work produced (gross IMEP). The brake thermal efficiency is high (34.4%), and the NOx and soot emissions are ultra-low (0.18 g/kW-hr and FSN of 0.0, respectively), relative to diesel combustion. For reference, the stock Euro IV Opel calibration of the diesel engine used in this study yields a brake thermal efficiency of 33.4%, BSNOx emissions of 1.2 g/kW-hr, FSN of 1.0, PPRR of 3 bar/°CA, and a combustion efficiency of 99.5% at 2000 rpm and 4.0 bar BMEP [22]. However, despite the high efficiency and low NOx and soot emissions, this PPC operating strategy has challenges with low combustion efficiency and high PPRR, particularly for the light-duty engine marketplace where combustion noise is an important metric.

Summary & Conclusions

The main focus of this study was to characterize the effect of the pilot (i.e., first) direct injection timing on gasoline “majority-premixed” PPC. The operating strategy aims to premix the majority of the fuel through the first direct injection and use a main injection late during the compression stroke to create a stratified charge before ignition.

The study was conducted using a modern light-duty diesel engine with wide included angle common rail injectors, a variable geometry turbocharger, variable swirl actuation, and a piston suited for premixed combustion concepts. Of the pilot injection timings investigated, four occurred while the intake valve was open and two occurred after the intake valve had closed (IVC = -132° ATDC). The study was conducted using a low octane, gasoline boiling range fuel (research octane number of 68).

It was found that the early pilot injection timings during the intake stroke yielded the most favorable results. The most notable implication of having the pilot injection during the intake stroke was a 30% reduction in HC emissions compared with later pilot injection timings. This is thought to occur because of the high in-cylinder turbulence levels and thus mixing rates that are generated by the intake process. The latest pilot injection timings (126° and -91° ATDC) occur after the intake valve had closed, when the chamber is expected to be relatively quiescent and mixing rates are low. These injection events are going to target the cylinder liner and most likely lead to fuel impingement on the liner, resulting in high HC emissions. On the contrary, the pilot injection timings that occur while the intake valve is open most likely experience faster breakup, vaporization, and mixing with the incoming air. These timings might not impinge on the liner and thus lead to more complete combustion.

The pilot injection timing sweep was conducted at various swirl ratios, injection pressures, and intake pressures. The aforementioned reduction in HC emissions was consistent for all engine operating conditions investigated. By combining the optimal conditions from the various parametric studies it was found that majority premixed PPC operation at 2000 rpm and 4.0 bar BMEP can yield diesel-like brake thermal efficiencies or higher while producing ultra-low NOx (less than 0.2 g/kW-hr) and soot emissions (FSN of 0.00).

For majority premixed gasoline PPC operation, challenges still exist with pressure rise rates (i.e., combustion noise), combustion efficiency, and combustion controllability. Future studies will focus on understanding the impact of various types of gasoline on PPC operation in multi-cylinder light-duty engines and how the efficiency, pressure rise rate, stability, and controllability are affected.

Acknowledgements

The authors would like to thank Jim Szybist, Derek Splitter, Ben Lawler, and Brian Kaul from Oak Ridge National Laboratory for many helpful discussions about low temperature combustion with gasoline. The fuel used in this study was provided by Chevron.

Disclaimer

This manuscript has been authored by UT-Battelle, LLC under Contract No. DE-AC05-00OR22725 with the U.S. Department of Energy. The United States Government retains and the publisher, by accepting the article for publication, acknowledges that the United States Government retains a non-exclusive, paid-up, irrevocable, world-wide license to publish or reproduce the published form of this manuscript, or allow others to do so, for United States Government purposes. The Department of Energy will provide public access to these results of federally sponsored research in accordance with the DOE Public Access Plan (http://energy.gov/downloads/doe-public-access-plan).

References

[1] Najt, P. M., and Foster, D. E., "Compression-Ignited Homogeneous Charge Combustion," SAE Technical Paper 830264, 1983, doi: 10.4271/830264.

[2] Manente, V., Johansson, B., and Tunestal, P., "Partially Premixed Combustion at High Load using Gasoline and Ethanol, a Comparison with Diesel," SAE Technical Paper 2009-01-0944, 2009, doi: 10.4271/2009-01-0944.

[3] Manente, V., Johansson, B., Tunestal, P., and Cannella, W., "Effects of Ethanol and Different Type of Gasoline Fuels on Partially Premixed Combustion from Low to High Load," SAE Technical Paper 2010-01-0871, 2010, doi: 10.4271/2010-01-0871.

[4] Chadwell, C., Alger, T., Roberts, C., and Arnold, S., "Boosting Simulation of High Efficiency Alternative Combustion Mode Engines," SAE Int. J. Engines, vol. 4, pp. 375–393, 2011, doi: 10.4271/2011-01-0358.

[5] Suresh, A., Langenderfer, D., Arnett, C., and Ruth, M., "Thermodynamic Systems for Tier 2 Bin 2 Diesel Engines," SAE Int. J. Engines, vol. 6, no. 1, pp. 167–183, 2013, doi: 10.4271/2013-01-0282.

[6] Ciatti, S., Johnson, M., Adhikary, B. Das, Reitz, R., and Knock, A., "Efficiency and Emissions performance of Multizone Stratified Compression Ignition Using Different Octane Fuels," SAE Technical Paper 2013-01-0263, 2013, doi: 10.4271/2013-01-0263.

[7] Dec, J. E., Yang, Y., and Dronniou, N., "Boosted HCCI - Controlling Pressure-Rise Rates for Performance Improvements using Partial Fuel Stratification with Conventional Gasoline," SAE Int. J. Engines, vol. 4, no. 1, pp. 1169–1189, 2011, doi: 10.4271/2011-01-0897.

[8] Ra, Y., Loeper, P., Reitz, R., Andrie, M., Krieger, R., Foster, D., Durrett, R., Gopalakrishnan, V., Plazas, A., Peterson, R., and Szymkowicz, P., "Study of High Speed Gasoline Direct Injection Compression Ignition (GDICI) Engine Operation in the LTC Regime," SAE Int. J. Engines, vol. 4, no. 1, pp. 1412–1430, 2011, doi: 10.4271/2011-01-1182.

[9] Loeper, P., Ra, Y., Adams, C., Foster, D., Ghandhi, J., Andrie, M., Krieger, R., and Durrett, R., "Experimental Investigation of Light-Medium Load Operating Sensitivity in a Gasoline Compression Ignition (GCI) Light-Duty Diesel Engine," SAE Technical Paper 2013-01-0896, 2013, doi: 10.4271/2013-01-0896.

[10] Sellnau, M. C., Sinnamon, J., Hoyer, K., and Husted, H., “Full-Time Gasoline Direct-Injection Compression Ignition (GDCI) for High Efficiency and Low NOx and PM,” SAE Int. J. Engines, vol. 5, pp. 300–314, 2012, doi: 10.4271/2012-01-0384.

[11] Dempsey, A. B., Walker, N. R., Gingrich, E., and Reitz, R. D., “Comparison of Low Temperature Combustion Strategies for Advanced Compression Ignition Engines with a Focus on Controllability,” Combustion Science and Technology, vol. 186, no. 2, pp. 210–241, 2013, doi: 10.1080/00102202.2013.858137.

[12] Hanson, R., Curran, S., Wagner, R., Kokjohn, S., Splitter, D., and Reitz, R., “Piston Bowl Optimization for RCCI Combustion in a Light-Duty Multi-Cylinder Engine,” SAE Int. J. Engines, vol. 5, no. 2, pp. 286–299, 2012, doi: 10.4271/2012-01-0380.

[13] Dempsey, A. B., Walker, N. R., and Reitz, R. D., “Effect of Piston Bowl Geometry on Dual-Fuel Reactivity Controlled Compression (RCCI) in a Light-Duty Engine Operated with Gasoline/Diesel and Methanol/Diesel,” SAE Int. J. Engines, vol. 6, no. 1, pp. 78–100, 2013, doi: 10.4271/2013-01-0264.

[14] Dempsey, A. B., “Dual-Fuel Reactivity Controlled Compression Ignition (RCCI) with Alternative Fuels,” University of Wisconsin-Madison PhD Dissertation (Mechanical Engineering), 2013.

[15] Yang, Y., Dec, J., Dronniou, N., and Cannella, W., “Boosted HCCI Combustion Using Low-Octane Gasoline with Fully Premixed and Partially Stratified Charges,” SAE Int. J. Engines, vol. 5, pp. 1075–1088, 2012, doi: 10.4271/2012-01-1120.

[16] Wang, M., Lee, H., and Molburg, J., “Allocation of Energy Use in Petroleum Refineries to Petroleum Products: Implications for Life-Cycle Energy Use and Emission Inventory of Petroleum Transportation Fuels,” The International Journal of Life Cycle Assessment, vol. 9, no. 1, pp. 34–44, 2003, doi: http://dx.doi.org/10.1065/lca2003.07.129.

[17] Manente, V., Johansson, B., and Cannella, W., “Gasoline partially premixed combustion, the future of internal combustion engines?,” International Journal of Engine Research, vol. 12, no. 3, pp. 194–208, 2011, doi: 10.1177/1468087411402441.

[18] Dec, J. E., “Advanced compression-ignition engines—understanding the in-cylinder processes,” Proceedings of the Combustion Institute, vol. 32, no. 2, pp. 2727–2742, 2009, doi: 10.1016/j.proci.2008.08.008.

[19] Heywood, J. B., Internal Combustion Engine Fundamentals. McGraw-Hill Book Company, 1988, pp. 338–339.

[20] Kokjohn, S. L., Hanson, R. M., Splitter, D. A., Kaddatz, J. , and Reitz, R. D., “Fuel Reactivity Controlled Compression Ignition (RCCI) Combustion in Light- and Heavy-Duty Engines,” SAE Int. J. Fuels Lubr., vol. 4, no. 1, pp. 360–374, 2011, doi: 10.4271/2011-01-0357.

[21] Chen, S., and Flynn, P., “Development of a Single Cylinder Compression Ignition Research Engine,” SAE Technical Paper 650733, 1965, doi: 10.4271/650733.

[22] Curran, S., Hanson, R., Wagner, R., and Reitz, R., “Efficiency and Emissions Mapping of RCCI in a Light-Duty Diesel Engine,” SAE Technical Paper 2013-01-0289, 2013, doi: 10.4271/2013-01-0289.